

Triangular metallic gratings for large absorption enhancement in thin film Si solar cells

Enes Battal,^{1,*} Taha Alper Yogurt,¹ Levent Erdal Aygun,^{1,2} and Ali K. Okyay^{1,2,3}

¹Department of Electrical and Electronics Engineering, Bilkent University, Ankara 06800, Turkey

²UNAM- National Institute of Materials Science and Nanotechnology Bilkent University, Ankara 06800, Turkey

³aokyay@ee.bilkent.edu.tr

*enesbattal@gmail.com

Abstract: We estimate high optical absorption in silicon thin film photovoltaic devices using triangular corrugations on the back metallic contact. We computationally show 21.9% overall absorptivity in a 100-nm-thick silicon layer, exceeding any reported absorptivity using single layer gratings placed on the top or the bottom, considering both transverse electric and transverse magnetic polarizations and a wide spectral range (280 – 1100 nm). We also show that the overall absorptivity of the proposed scheme is relatively insensitive to light polarization and the angle of incidence. We also discuss the implications of potential fabrication process variations on such a device.

©2012 Optical Society of America

OCIS codes: (250.5403) Plasmonics; (040.5350) Photovoltaic; (050.2770) Gratings; (240.6680) Surface plasmons; (350.6050) Solar energy.

References and links

1. W. Koch, A. L. Endrös, D. Franke, C. Häbeler, J. P. Kalejs, and H. J. Möller, "Bulk crystal growth and wafering for PV," in *Handbook of Photovoltaic Science and Engineering* (John Wiley & Sons, 2005), pp. 205–254.
2. C. Rockstuhl, S. Fahr, and F. Lederer, "Absorption enhancement in solar cells by localized plasmon polaritons," *J. Appl. Phys.* **104**(12), 123102 (2008).
3. C. Rockstuhl and F. Lederer, "Photon management by metallic nanodiscs in thin film solar cells," *Appl. Phys. Lett.* **94**(21), 213102 (2009).
4. R. A. Pala, J. White, E. Barnard, J. Liu, and M. L. Brongersma, "Design of plasmonic thin-film solar cells with broadband absorption enhancements," *Adv. Mater. (Deerfield Beach Fla.)* **21**(34), 3504–3509 (2009).
5. Y. A. Akimov, W. S. Koh, and K. Ostrikov, "Enhancement of optical absorption in thin-film solar cells through the excitation of higher-order nanoparticle plasmon modes," *Opt. Express* **17**(12), 10195–10205 (2009).
6. F.-J. Tsai, J.-Y. Wang, J.-J. Huang, Y.-W. Kiang, and C. C. Yang, "Absorption enhancement of an amorphous Si solar cell through surface plasmon-induced scattering with metal nanoparticles," *Opt. Express* **18**(S2 Suppl 2), A207–A220 (2010).
7. V. E. Ferry, M. A. Verschuuren, H. B. T. Li, R. E. I. Schropp, H. A. Atwater, and A. Polman, "Improved red-response in thin film a-Si:H solar cells with soft-imprinted plasmonic back reflectors," *Appl. Phys. Lett.* **95**(18), 183503 (2009).
8. W. Wang, S. Wu, K. Reinhardt, Y. Lu, and S. Chen, "Broadband light absorption enhancement in thin-film silicon solar cells," *Nano Lett.* **10**(6), 2012–2018 (2010).
9. M.-G. Kang, T. Xu, H. J. Park, X. Luo, and L. J. Guo, "Efficiency enhancement of organic solar cells using transparent plasmonic Ag nanowire electrodes," *Adv. Mater. (Deerfield Beach Fla.)* **22**(39), 4378–4383 (2010).
10. L. Yifen and K. Jaeyoun, "Grating-induced surface plasmon-polaritons for enhancing photon absorption in organic photovoltaic devices," in *OSA Technical Digest (CD) (Optical Society of America, 2010)*, CMAA5.
11. M. A. Sefunc, A. K. Okyay, and H. V. Demir, "Plasmonic backcontact grating for P3HT:PCBM organic solar cells enabling strong optical absorption increased in all polarizations," *Opt. Express* **19**(15), 14200–14209 (2011).
12. H. Shen, P. Bienstman, and B. Maes, "Plasmonic absorption enhancement in organic solar cells with thin active layers," *J. Appl. Phys.* **106**(7), 073109–073, 109–073105 (2009).
13. H. A. Atwater and A. Polman, "Plasmonics for improved photovoltaic devices," *Nat. Mater.* **9**(3), 205–213 (2010).
14. S. Vedraïne, P. Torchio, D. Duché, F. Flory, J. Simon, J. Le Rouzo, and L. Escoubas, "Intrinsic absorption of plasmonic structures for organic solar cells," *Sol. Energy Mater. Sol. Cells* **95**(Supplement 1), S57–S64 (2011).
15. W. Bai, Q. Gan, G. Song, L. Chen, Z. Kafafi, and F. Bartoli, "Broadband short-range surface plasmon structures for absorption enhancement in organic photovoltaics," *Opt. Express* **18**(S4 Suppl 4), A620–A630 (2010).

16. V. E. Ferry, L. A. Sweatlock, D. Pacifici, and H. A. Atwater, "Plasmonic nanostructure design for efficient light coupling into solar cells," *Nano Lett.* **8**(12), 4391–4397 (2008).
 17. M. A. Sefunc, A. K. Okyay, and H. V. Demir, "Volumetric plasmonic resonator architecture for thin-film solar cells," *Appl. Phys. Lett.* **98**(9), 093117 (2011).
 18. FDTD Solutions, Lumerical Solutions, Inc., Vancouver, British Columbia, Canada.
 19. E. D. Palik, *Handbook of Optical Constants of Solids* (Academic, 1985).
 20. H. Hoppe, N. S. Sariciftci, and D. Meissner, "Optical constants of conjugated polymer/fullerene based bulk-heterojunction organic solar cells," *Mol. Cryst. Liq. Cryst. (Phila. Pa.)* **385**(1), 113–119 (2002).
 21. E. Yablonovitch, "Statistical ray optics," *J. Opt. Soc. Am.* **72**(7), 899–907 (1982).
 22. K. X. Wang, Z. Yu, V. Liu, Y. Cui, and S. Fan, "Absorption enhancement in ultrathin crystalline silicon solar cells with antireflection and light-trapping nanocone gratings," *Nano Lett.* **12**(3), 1616–1619 (2012).
-

1. Introduction

Energy and environmental challenges fuel the need for highly efficient and low cost photovoltaics (PV). Even though conventional Silicon solar cells exhibit high quantum efficiencies, significant portion of the cost is associated with materials [1]. Therefore, thin film PV devices gathered the attention of PV community because of reduced amount of materials use, coupled, however, with reduced efficiency due to less active material. The use of plasmonic structures is promising to provide stronger light absorption in active layers of sub-wavelength thickness. Single layer of one- or two-dimensional rectangular or circular metallic nanogratings or nanoparticles placed at the top [2–6], bottom [7–11] or buried inside [12–14] the active layer have been extensively studied for improving the performance of both organic and inorganic thin film solar cells. In addition, several patterned back contact structures such as nanohole arrays [15] or hexagonal arrays [16] for thin film solar cells have also been demonstrated. Reported performance enhancements in Silicon-based thin-film PV devices, using single-layer plasmonic designs, have been limited to less than 30%. In our earlier work, a volumetric coupling of resonant modes was computationally shown to exceed the limit of enhancement provided by a single-layer metallic structure, with an increased challenge of fabrication [17].

In this work, we design and computationally analyze triangle-shaped nano-metallic gratings, and report the highest enhancement of absorptivity in Silicon thin film PV devices, using single layer gratings placed on the top or the bottom, considering both TE and TM polarizations and a wide spectral range (280 – 1100 nm). We investigate the effects of polarization and incidence angle of illumination on overall optical absorptivity. We calculate the overall absorptivity for the proposed structure and compare to reference structures.

2. Proposed structure and simulations

The proposed structure is a 100-nm-thick single crystalline Silicon (Si) absorbing layer sandwiched between 80-nm-thick silver (Ag) layer with triangular corrugations on the bottom and, 20-nm-thick indium-tin-oxide (ITO), transparent conducting electrode on the top, as illustrated in Fig. 1(a). The triangular corrugations on the bottom electrode are assumed to be penetrating into the active Si layer. We do not report the fabrication of such a structure, however, we assume that the corrugations are isosceles triangular prisms with 54.7° base angles, related to (111) crystal plane orientation of Silicon that can be obtained by anisotropic chemical etching. The structure is illuminated from the top with a plane wave, and all reflections and transmissions from surfaces are accounted for. The reference structure (dubbed as "bare") is chosen as the same stack of layers with identical thicknesses, except for the lack of corrugations, with a flat Ag back reflector, as depicted in Fig. 1(b). Periodic metallic grating is designed on the back contact to avoid or minimize losses due to surface reflections and ohmic losses in a top metal surface. Triangular shape of the gratings is used to leverage strong enhancements in both TE and TM polarizations with the excitation of various optical as well as plasmonic modes and their coupling. Triangular gratings buried into the active layers allow the exploitation of the near field by placing the absorbing layer in close proximity of the enhanced fields.

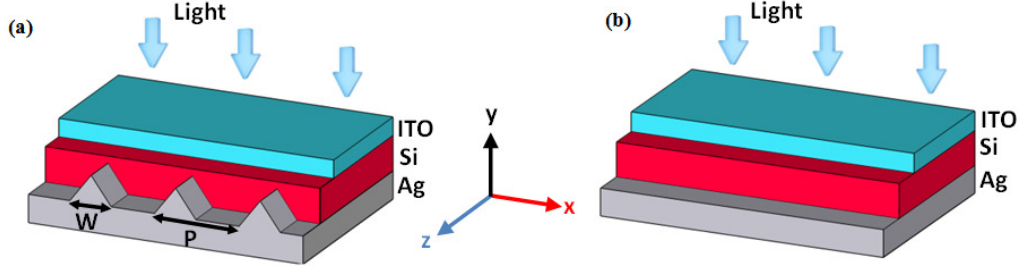


Fig. 1. (a) Proposed structure with top contact (ITO), absorbing layer (Si) and back reflector (Ag) with triangular corrugations, with thicknesses 20 nm, 100 nm, and 80 nm, respectively. (b) Bare structure identical to proposed structure except for the lack of the triangular corrugations. The arrows indicate the direction of illumination.

We performed two-dimensional simulations using FDTD Solutions, by Lumerical Inc. [18] for both TE and TM polarizations under AM1.5G solar radiation. We have optimized base width (W) and period (P) of triangular prism shaped gratings as defined in Fig. 1(a). Computations were performed on a single unit cell with periodic boundary conditions set in x -axis, and perfectly matched layers (PML) at the top and bottom of the structure in y -axis. We set square meshes with 1 nm grid spacing on the triangles, and 2nm grid spacing elsewhere. We tested the effects of different grid sizes and found that the results vary less than 5% below 1 nm grid size. In our computations, we assumed experimentally obtained data for optical properties (refractive index, absorption) of Si, Ag [19, 20] and ITO [20] layers in the 280 nm $< \lambda < 1100$ nm spectral range where Si has finite absorption. The optical absorptivity of the structure at a given wavelength (λ) is calculated by Eq. (1) and the overall absorptivity of the structure is calculated by the average absorptivity considering both TE and TM polarization as given by Eq. (2).

$$A = \omega \times \text{Im}(\epsilon) \oint |E|^2 dV \quad (1)$$

$$A_{\text{OVERALL}} = \frac{\int_{280\text{nm}}^{1100\text{nm}} \frac{(A_{\text{TM}} + A_{\text{TE}})}{2} \times \text{AM1.5G}(\lambda) d\lambda}{\int_{280\text{nm}}^{1100\text{nm}} \text{AM1.5G}(\lambda) d\lambda} \quad (2)$$

3. Results and discussion

The assumed geometry of the structures dictates a fixed relation between base width and height of the triangular corrugations, therefore, the effect of base width on overall absorptivity is investigated. Figure 2 plots overall absorptivity vs. base width and period of the corrugations. Overall absorptivity increases with the base width of the corrugations, despite decreasing total volume of Silicon absorbing layer. As the base width increases, both plasmonic and optical resonances provide higher field enhancements in Silicon layer. An overall absorptivity of 21.9% is observed with an optimized design as shown by the arrow in Fig. 2. This is the highest overall absorptivity for 100-nm-thick single crystal Silicon active layer devices with single layer gratings considering both TE and TM polarizations and a wide spectral range (280 – 1100 nm). The reference structure (Fig. 1(b)) exhibits an overall absorptivity of 16%. Thus, an overall absorptivity enhancement (defined with respect to the reference) by a factor of 38% is obtained with our optimum design. Both TE-polarized (53.6%) and TM-polarized (46.4%) illumination contributes to the total absorptivity.

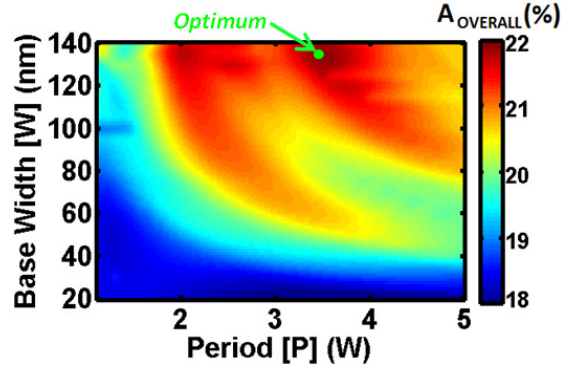


Fig. 2. Overall absorptivity (%) as a function of base width (W) of the triangle and period (P) of the corrugations. Period is expressed as multiples of base width (W).

The spectral response of the proposed structure for both TE- and TM-polarized light, are plotted for base width 135 nm in Fig. 3, with respect to period, P. Figure 3 effectively exhibits the dispersion characteristics of the proposed structure. In Fig. 3(a), plotted for TM-polarized illumination, S_1 , S_2 and S_3 correspond to the excited surface plasmon polariton (SPP) mode of different grating orders. The vertical dashed lines in Fig. 3(a) and 3(b) indicate the optimum structure. C_1 and C_2 in Fig. 3(b), correspond to the orders of cavity modes. Figure 3(c) plots the spectral absorptivity for the optimized design, exhibiting relatively broad absorption characteristics. In Fig. 4, we calculate the spectral distribution of total absorbed photons

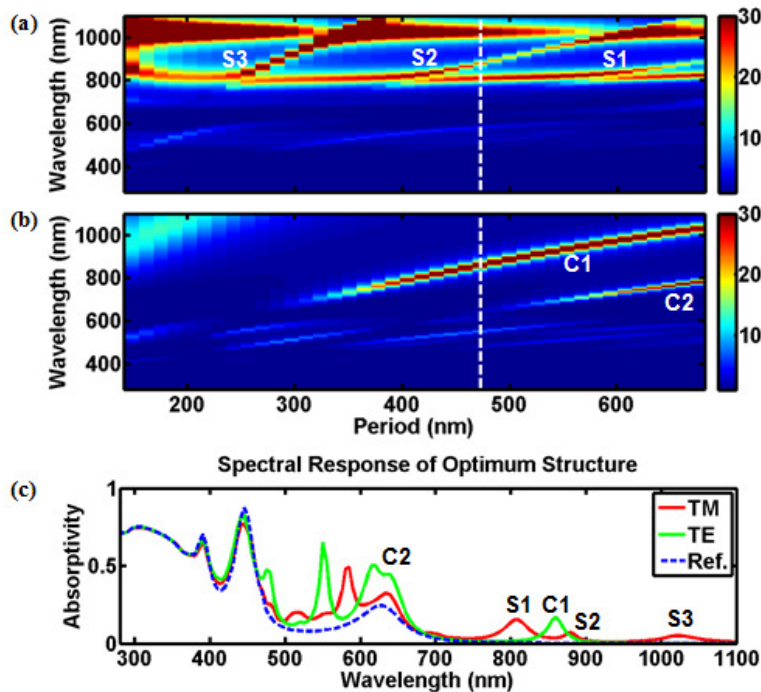


Fig. 3. Absorptivity enhancement as a function of period (P) and wavelength when $W = 135$ nm for (a) TM and (b) TE polarizations. (c) Spectral response of optimum structure ($W = 135$ nm and $P = 470$ nm).

for both TM and TE polarized light for the optimum structure. The absorption enhancement in our design is prominent in relatively longer wavelengths. The optimum structure exhibits 49.3% enhancement in the overall number of absorbed photons which correspond to a same

rate of increase in short circuit current density assuming 100% charge carrier collection efficiency. In addition, Yablonovitch limit [21, 22] is exceeded mainly for particular spectral segment, 550-650nm.

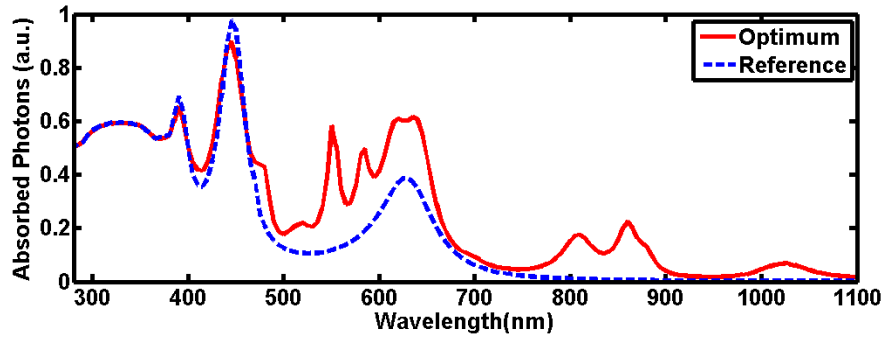


Fig. 4. Spectral distribution of absorbed photon count for the optimum and reference structure considering both TM and TE illuminations.

For the optimum structure, the electric field (E-field) profiles corresponding to $\lambda = 805$ nm and $\lambda = 580$ nm (TM-polarized illumination) and to $\lambda = 855$ nm and $\lambda = 550$ nm (TE-polarized illumination) are shown in Fig. 5. The E-field profile in Fig. 5(a), corresponding to S_1 position, is due to strong excitation of surface plasmon polaritons at the Ag/Si interface of the triangular gratings. In Fig. 5(b), a coupling between the excited surface plasmon resonance and Fabry-Perot resonance modes is observed at $\lambda = 580$ nm. Despite TM-polarized illumination, the field enhancement is mainly due to the presence of Fabry-Perot resonance as the excited surface plasmons are weak in this case. Since the proposed structure is periodic in one dimension and infinitely long in the perpendicular direction, plasmonic modes are not excited by TE-polarized light. In Fig. 5(c), the excited cavity mode is demonstrated with its E-field profile for $\lambda = 855$ nm for TE polarized light. Coupling between waveguide and cavity

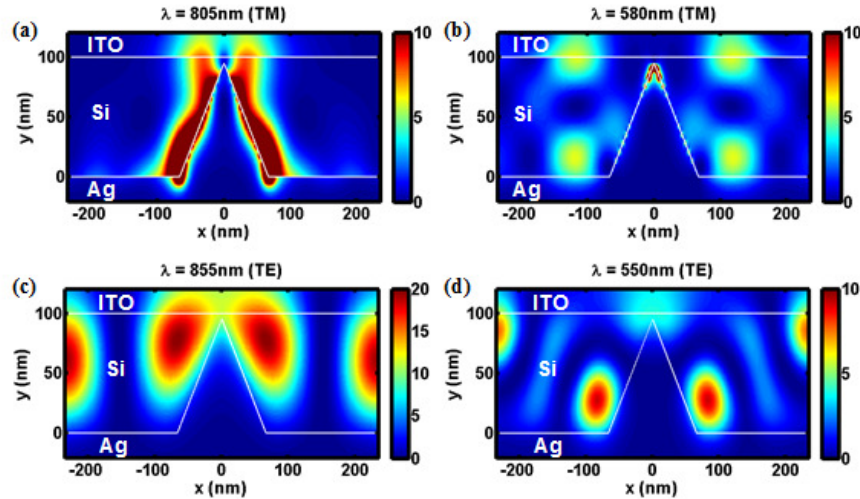


Fig. 5. E-field profile of the optimum structure at (a) $\lambda = 805$ nm (b) $\lambda = 580$ nm under TM polarization illumination and (c) at $\lambda = 855$ nm and (d) at $\lambda = 550$ nm under TE illumination.

modes is observed for $\lambda = 550$ nm as shown in Fig. 5(d). We plot the E-field profiles for $P = 404$ nm with $\lambda = 490$ nm and 520 nm in addition to $P = 470$ nm with $\lambda = 550$ nm, in Fig. 6(a), 6(b), 6(c), respectively. In Fig. 6(a), we observe a waveguide mode and in Fig. 6(b), we

observe a cavity mode corresponding to a standing wave between the sides of the triangular prism shape and the top surface of the silicon layer. When the period of the structure is changed to the optimum value ($P = 470\text{nm}$), a hybridized mode is observed due to coupling of these two modes, as seen in Fig. 6 (c).

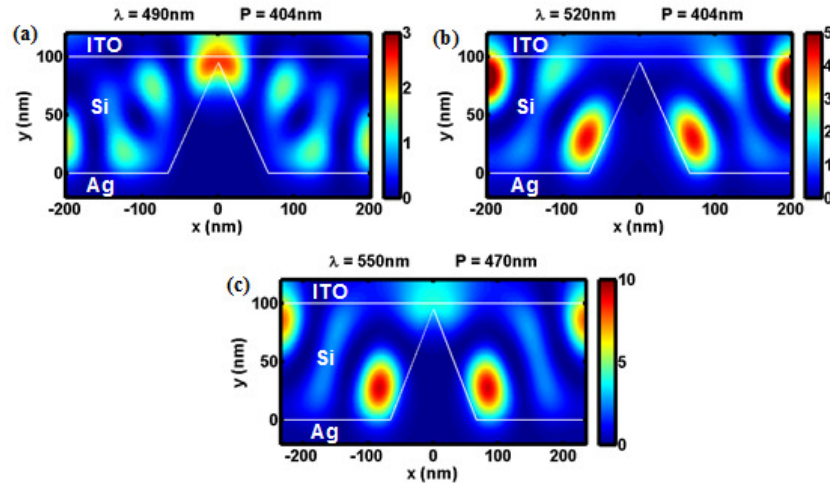


Fig. 6. E-field profile of the structure with 404 nm period at (a) $\lambda = 490\text{ nm}$ (b) $\lambda = 520\text{ nm}$ and optimum structure at (c) at $\lambda = 550\text{ nm}$ under TE polarization illumination.

The performance of a thin film solar cell with respect to illumination angle is very important because the solar illumination reaches the surface as a scattered illumination. We investigate the optimum design under different incidence angles. Figure 7(a) plots the overall absorptivity enhancement with respect to the incidence angle. Proposed triangular corrugations sustain large enhancement factors (33.8%-43.3%) up to relatively wide incidence angles. We also investigate the polarization dependence of the overall absorptivity as plotted in Fig. 7(b). For this purpose, computations were performed by rotating the light source from TE (0°) to TM (90°) polarization, where angles in Fig. 7(b) imply the angle between the direction of E-field and gratings. Our structure performs high polarization insensitivity such that we observe a maximum of $\pm 0.8\%$ variation in the overall absorptivity from the optimum value (21.9%). This is attributed to similar field enhancement contributions from both TE and TM polarizations.

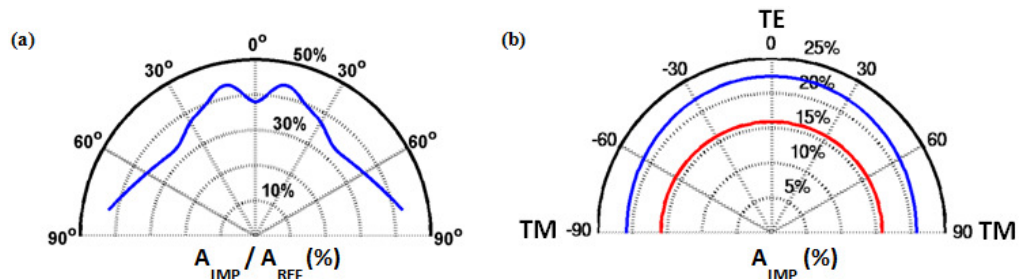


Fig. 7. (a) Incidence angle vs overall absorptivity enhancement for the optimum structure (b) Polarization dependence of overall absorptivity of the optimum structure (blue curve) and the reference structure (red curve).

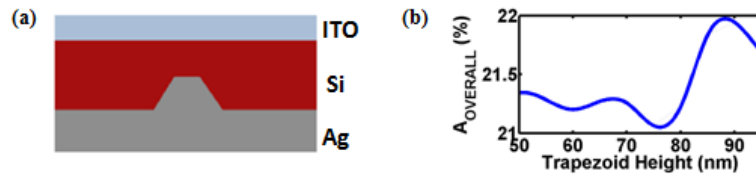


Fig. 8. (a) Cross section of device with truncated triangular corrugations (b) Overall absorptivity as a function of trapezoid height, optimized for each height.

Despite certain fabrication challenges of our proposed structure, we theoretically investigate potential process limitations and their implication on device performance. In a practical production scenario, realization of sharp tips may prove difficult; therefore, we have investigated a truncated trapezoidal prism shaped gratings, illustrated in Fig. 8(a). The base width (135 nm) and grating period (470 nm) of optimized structure are fixed and the height of the trapezoid is changed in computations. Overall absorptivity as a function of trapezoid height is depicted in Fig. 8(b). As seen in the figure, the overall absorptivity changes less than 1.1% while the height of the trapezoid is varied from 95 nm (ideal triangular shape of optimized design) down to 50 nm.

In order to address leakage currents, an oxide layer can be desirable between the ITO top contact and Silicon active layer [4]. We repeat the simulations for optimized structure including an interfacial SiO_2 layer between ITO and Silicon as depicted in Fig. 9(a), for various SiO_2 layer thicknesses. The results shown in Fig. 9(b) exhibit a slight increase in overall absorptivity with SiO_2 layer thickness. Figure 9(c) plots spectral absorptivity for different SiO_2 thicknesses, and the increase in overall absorptivity is attributed to antireflection from the surface and stronger confinement of optical modes, especially in the 280-500 nm spectral range.

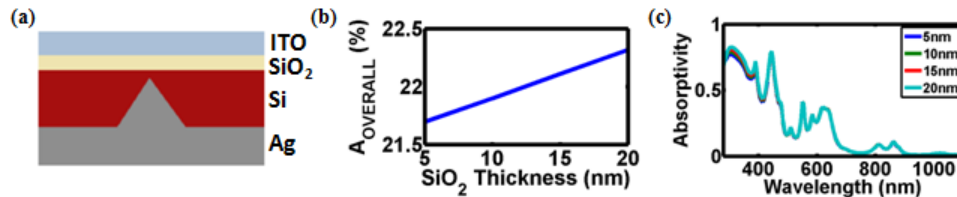


Fig. 9. (a) Cross section of device with interfacial SiO_2 layer between Si and ITO. (b) Overall absorptivity as a function of SiO_2 thickness (c) Spectral absorptivity of device with interfacial SiO_2 as a function of oxide thickness.

4. Conclusion

We propose and computationally investigate triangular prism shaped gratings on overall absorptivity of Silicon thin film PV devices. Such a structure exploits surface plasmon polariton and localized surface plasmon modes in addition to optical resonances such as waveguide modes and Fabry-Perot resonances. We estimate overall absorptivities as high as 21.9% under AM1.5G illumination including both polarizations, highest with single crystalline Silicon active layer devices with single layer gratings. In addition, we also estimate low angular dependency, providing very high enhancements for a wide range of incidence angles. We also computationally investigate impacts of potential fabrication variations in overall device performance, promising relative insensitivity.

Acknowledgments

This work was supported by TUBITAK 108E163, 109E044, EU FP7 PIOS 239444. The authors acknowledge TUBITAK BIDEF. The numerical calculations reported in this paper were performed at TUBITAK ULAKBIM, High Performance and Grid Computing Center (TR-Grid e-Infrastructure).